JACS
JOURNAL OF THE AMERICAN CHEMICAL SOCIETY

ARTICLE

pubs.acs.org/JACS

Proton Transfer and Dissociation of GlyLysH$^+$ following O−H and N−H Stretching Mode Excitations: Dynamics Simulations

Michaela Shmilovits-Ofir[†] and R. Benny Gerber[*,†,‡]

[†]Department of Physical Chemistry and the Fritz Haber Research Center, The Hebrew University, Jerusalem 91904, Israel
[‡]Department of Chemistry, University of California, Irvine, California 92697-2025, United States

Supporting Information

ABSTRACT: Proton transfer and dissociation processes following excitation of the OH or NH stretching modes of the proton-bound complex GlyLysH$^+$ are studied by classical trajectories. "On the fly" simulations with the PM3 semiempirical electronic structure method for the potential surface are used. Initial conditions are sampled to correspond to the v=1 excited state of the OH or NH stretching modes. Five different conformers of the complex are studied as initial structures. The main findings are (1) Photoinduced proton transfer is on the picosecond time scale. (2) Proton transfer is much faster than the processes of dissociation. (3) Proton transfer involves different sites. Most trajectories show sequences of two proton transfer events. (4) The proton transfer events show high selectivity with regard to the initially excited vibration and the initial structure. (5) Photodissociation of the complex occurs on a typical time scale of 100 ps. (6) Conformational transitions are found to be often faster than proton transfer. These results have implications for the mass spectrometry of complexes, for dynamics of proton wires, and for proton migration in proteins.

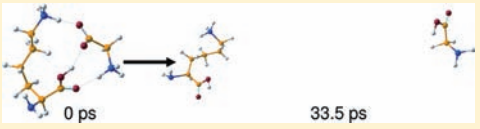

1. INTRODUCTION

Proton transfer plays a critical role in the function of proteins and peptides.[1] A wealth of information and insights on proton transfer processes was obtained in exploration of related but smaller biological molecules.[2−14] This motivates the present study, in which proton transfer is studied in a small but realistic proton bound complex of amino acids.

Proton bound dimers of amino acids are species of very considerable interest. These species are very useful model systems for studies of proton mobility and their interactions in peptides and proteins. They are studied extensively by mass spectrometry, shedding light on questions regarding proton affinities and bond dissociation energies,[15] structural effects of competitive charging of heteroatoms,[16] the excited-state dynamics associated with isomerization,[17] and the necessary conditions for the stabilization of gas phase zwitterionic species.[16,18] The molecular mechanism for proton conduction along hydrogen-bonded chains of water molecules (proton wires) has been studied extensively, since the control of proton fluxes across biomembranes constitutes one of the fundamental life processes.[19−23] Another example involves the protonated Ala_2H^+ (alanine$_2$-H$^+$) and Ala_3H^+ (alanine$_3$-H$^+$), which were studied extensively for understanding the relationship between IR-MPD (infrared multiphoton dissociation) experimental features and the molecular structural and dynamical properties, including vibrational anharmonicities.[24] In these studies, the spectra of the two proton bound complexes calculated from finite temperature DFT (density functional theory) based dynamics were found to be in very good agreement with the experiments.[25−29] Despite the progress in the studies of proton transfer, theoretical analysis of the processes taking place during MS is still largely missing, especially of the migration route of the protons and of conformational changes and dissociation pathways related to proton transfer.

In the present study, we focus on the proton-bound dimer of amino acids GlyLysH$^+$ (glycine-lysine-H$^+$). That system was studied previously experimentally as well as computationally by Oh et al.,[30] who used an electrospray ionization technique to prepare the species. They found that the glycine/lysine heterodimer has two similar lowest energy isomers in which the glycine is zwitterionic. In that study, NH and OH stretches were excited, raising the question as to what is the role of the excitation type in the process.[30] Adesokan et al.[13] carried out anharmonic frequency calculations for this system, reaching the conclusion that agreement with the measured spectra supports the structure proposed by Oh et al.[30]

We present in this study classical trajectory simulations for fundamental vibrational excitation of selected different vibrational modes in five minimum energy conformers of GlyLysH$^+$. The potential energy surface (PES) used in the study was the semiempirical PM3 (parameterized model number 3). Through dynamics simulations aspects this study explores the role of vibrational excitation in proton transfer, dissociation, and conformational changes. A question that seems completely open at present are the dynamical processes that take place upon excitation, of an N−H or an O−H stretch, as in the experiments of Oh et al.[30] This is at the focus of the present paper.

The outline of this paper is as follows: in section 2, we present an overview of the system and the various methods we use in this

Received: June 17, 2011
Published: August 30, 2011

dx.doi.org/10.1021/ja205634b | J. Am. Chem. Soc. 2011, 133, 16510–16517

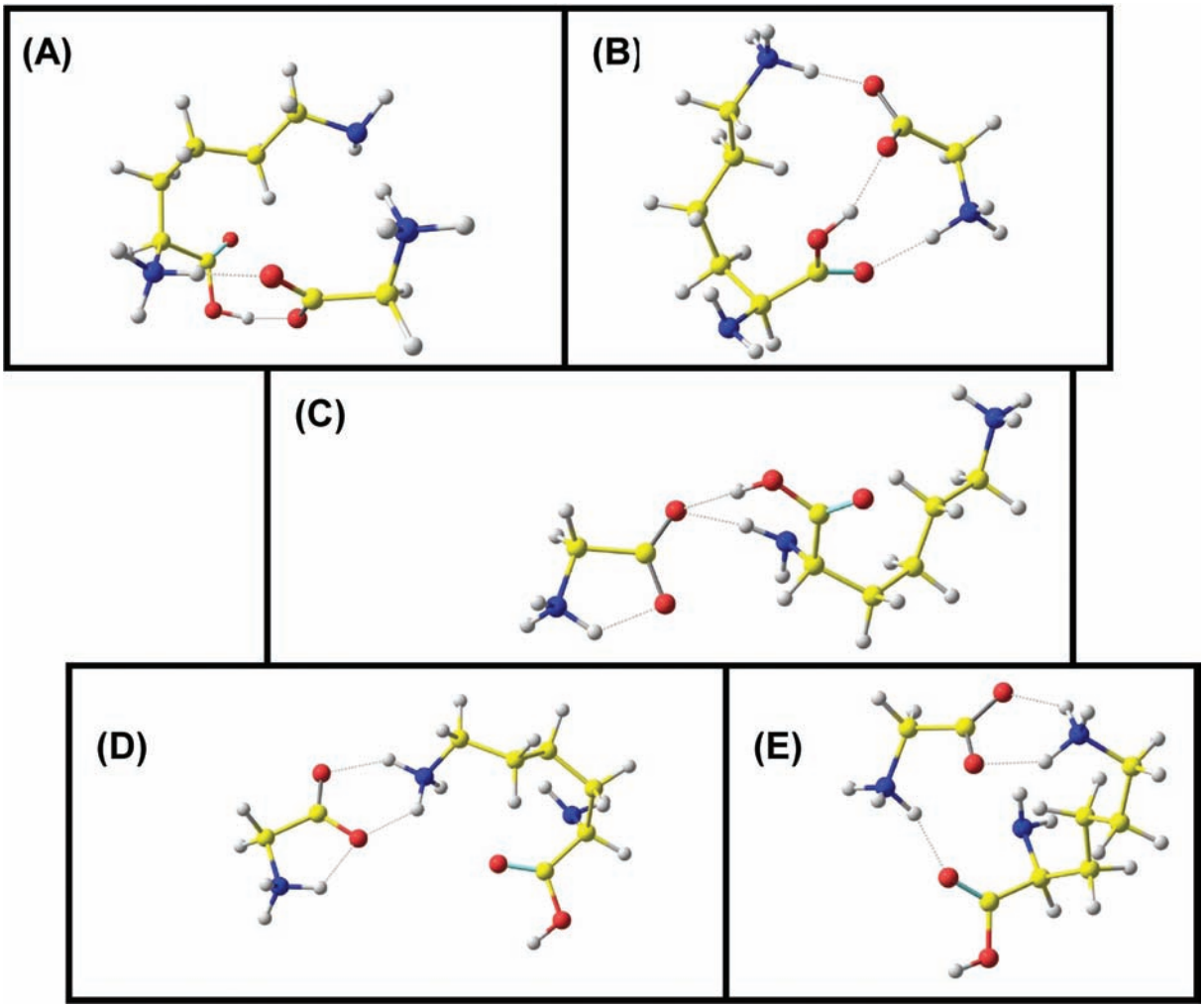

Figure 1. Optimized PM3 structures of five $GlyLysH^+$ conformers: (A) conformer 1, (B) conformer 2, (C) conformer 3, (D) conformer 4, and (E) conformer 5.

work to explore the conformational transitions. The results are presented and discussed in section 3. Finally, in section 4, concluding remarks are presented.

2. SYSTEM AND METHODOLOGY

2.1. System. $GlyLysH^+$ was studied previously by Adesokan et al.,[13] who carried out anharmonic frequency calculations by the VSCF (vibrational self-consistent field) method. They used an improved PM3 semiempirical electronic structure potential by fitting ab initio MP2 (second-order Møller−Plesset perturbation theory) frequencies at the harmonic level. They found good agreement between the computed anharmonic vibrational frequencies and the experiment.[13] From a structural point of view, Rajabi and Fridgen found that the homogeneous proton bound dimers of glycine, alanine, and valine, as well as the mixed glycine/alanine proton bound dimer, were nonzwitterionic.[31] On the other hand, several other theoretical calculations for the glycine/lysine complexes found that the glycine is a zwitterion.[15,32]

In the study by Oh et al.,[30] the authors computed two minimum energy structures of $GlyLysH^+$, and in both of which the glycine was a zwitterion. The isomer with the protonated terminal NH_2 group of lysine was higher in energy by 8.4 kJ/mol than the isomer with the protonated nonterminal NH_2 group of lysine. The spectrum of the heterodimer $GlyLysH^+$ is far more intense than that of Gly_2H^+ or Lys_2H^+. The dissociation energies of amino acid protonated dimers decrease linearly with the difference in the proton affinities of the components.[30]

2.2. Potential Energy Surface (PES). Force field potentials, such as AMBER (assisted model building with energy refinement), OPLS (optimized potentials for liquid simulations) and MMFF94 (Merck molecular force field), are the most extensively applied tools for investigating large biological molecules.[33−36] Although these force fields are easily used and computationally fast, validity for proton transfer cannot be expected, since, at least in their standard versions, they were not parametrized for such applications. Another disadvantage is that the vibrational frequency calculations using the empirical force fields have shown that both the harmonic parts of the potentials and especially the anharmonic couplings are inadequately described.[37,38] On the other hand, ab inito potentials are computationally demanding and applicable only for relatively small biological building blocks.[38,39] Since ab initio potentials are computationally expensive, we apply the PM3 semiempirical potential for the MD simulations. Although calculations with Car−Parinnello[27] were conducted previously for similar systems, we find PM3 much more convenient and efficient for running large numbers of trajectories. Previously, it was shown that with the proper adjustments, PM3 potentials gave vibrational frequencies similar to ab initio methods for several classes of biological molecules.[37,38,40] Further, PM3 potentials were employed for simulations of other small molecules, e.g., in the study of energy transfer and chemical processes.[41−43]

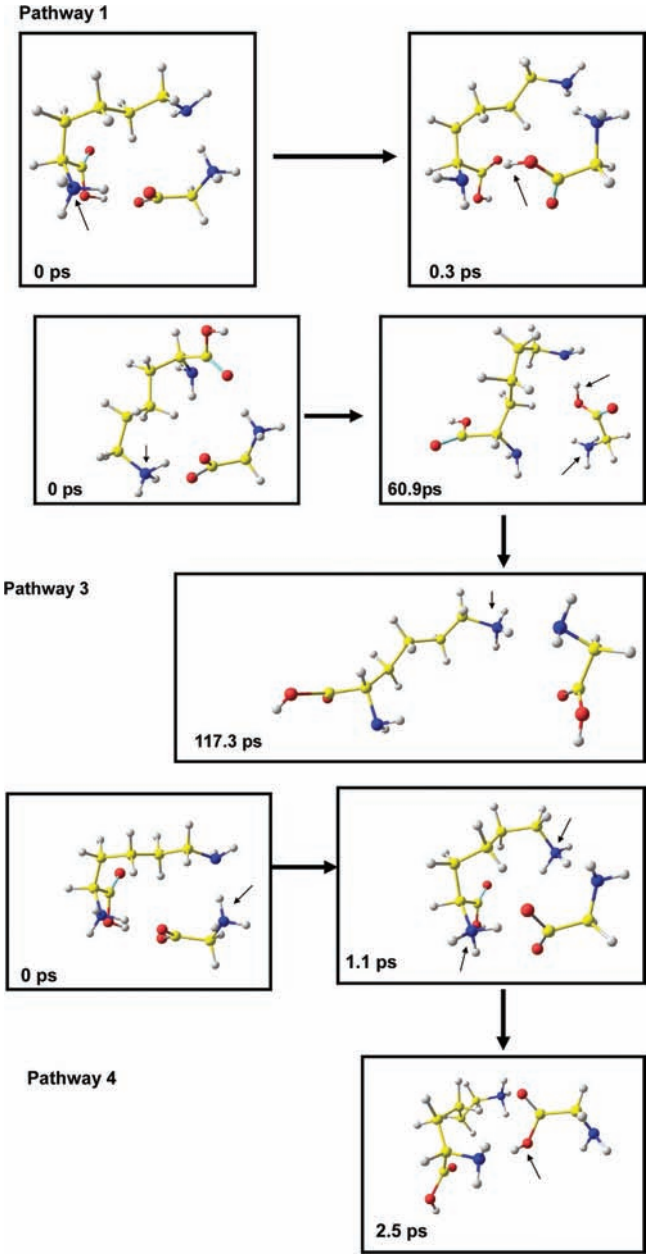

Figure 2. Three examples of proton transfer pathways found in the dynamics of different excitations of conformers (snapshots of different trajectories).

Shemesh et al. used PM3 in simulations of photoionization dynamics of tryptophan and found intramolecular hydrogen-transfer processes.[44] A justification for the present system is the following: We computed several structures of GlyLysH$^+$ with PM3 and MP2/DZV and found good agreement of the structural properties; thus, it is reasonable to assume that also the dynamics obtained using PM3 may be valid. Our claim of the validity of PM3 obviously applies only for the structures studied here, for which tests and comparisons with MP2 were carried out. In the present study, all the calculations of the initial structures and the MD simulations were performed using the electronic structure package GAMESS (general atomic and molecular electronic structure system).[45]

2.3. On-the-Fly Molecular Dynamics (MD) Simulations. We use "on-the-fly" MD simulations to investigate the dynamics following vibrational excitation in GlyLysH$^+$. At each very small time step of the trajectory, the PM3 potential is evaluated and the forces on the different atoms are computed. Newton's equations are used to update positions, velocities, and accelerations for each atom. The process is continued along the trajectories until the end of the simulations.[46−52] The self-consistent field convergence criterion in the electronic structure calculations used in this study is 10^{-11}.[42] We excited different modes (O−H and N−H stretching modes) for each conformer. We estimated that 20−25 trajectories are sufficient to describe the processes of interest with reasonable statistics for each different excitation. We started from 20 to 25 different initial geometries of five different local minimum energy conformers of GlyLysH$^+$, all sampled according to the v=1 excited state of the OH stretch or NH related modes. Each trajectory was computed for 45−250 ps (over this time scale, the processes of interest were found to take place) with the step size in the range of 0.06 fs. Since the most demanding in the MD simulations are the proton movements (for which the time scale of a typical motion is ∼20 fs), the use of such a short time step is reasonable.

2.4. Sampling the Initial Conditions for the MD Simulations. As a starting point, the minima of five conformers of GlyLysH$^+$ were computed using the PM3 semiempirical electronic structure method. These conformers were calculated in a search of structures similar to those found by Oh et al.[30,47] We further computed the normal vibrational modes of those conformers and the anharmonic energy levels and wave functions using the VSCF method. VSCF uses a separability approximation that reduces the problem of solving an N-dimensional vibrational Schrödinger equation for the N-mode system to solving N single-mode VSCF equations.[53,54] Then, the initial configurations are sampled from the VSCF wave function of the excited state of GlyLysH$^+$.

Several methods have been proposed in the literature for representing the distribution of classical positions and momenta for a given state.[42,55,56] The most common method to represent the distribution of the initial conditions for the MD simulations is the Wigner function, which provides a distribution of positions and momenta for a certain quantum-mechanical state.[42,44,56−59] Here, we used a different sampling method which was successfully applied by our group for similar processes.[43,60] The Wigner "distribution" function can have negative values in certain cases, but the method employed here is free of this problem.

The VSCF calculations include the potential surface along each normal mode Q_j and the interactions between all pairs of the normal modes. These interactions are computed on a square grid of 16 × 16 points for each pair of normal modes. The VSCF equations were solved numerically by the algorithm of Chaban et al.,[53,54] from which the wave function $\psi_v(Q_j)$ along each normal mode Q_j was obtained.

To investigate the averaged properties of the processes in GlyLysH$^+$, it is necessary to compute the weight of each trajectory. We computed the weight of each trajectory according to the following equation

$$\Psi(Q_1,\ldots,Q_N) = C\left|\psi_{1v}(Q_1)\prod_{j=2}^{N}\psi_j(Q_j)\right|^2 \quad (1)$$

where $(Q_1,\ldots,Q_N)$ denotes for the mass-weighted normal coordinates of a given initial structure. N is the total number of vibrational modes, $\psi_{1v}(Q_1)$ is the wave function of the OH or NH stretching modes at the vibrational state v, and $\Pi_{j=2}^{N}\psi_j(Q_j)$ is the product of the wave functions of the other 98 vibrational modes in GlyLysH$^+$. Finally, C is the normalization constant of the total vibrational wave function $\Psi(Q_1,\ldots,Q_N)$. In the present study, extensive statistical sampling was not used since the main motivation is to find time scales at a semiquantitative level for proton transfer, complex dissociation, and conformational changes.

The corresponding momentum values of the normal modes were calculated in the semiclassical approximation

$$P_j = \pm\,[2(E_{jv} - \bar{V}_j(Q_j))]^{1/2} \quad (2)$$

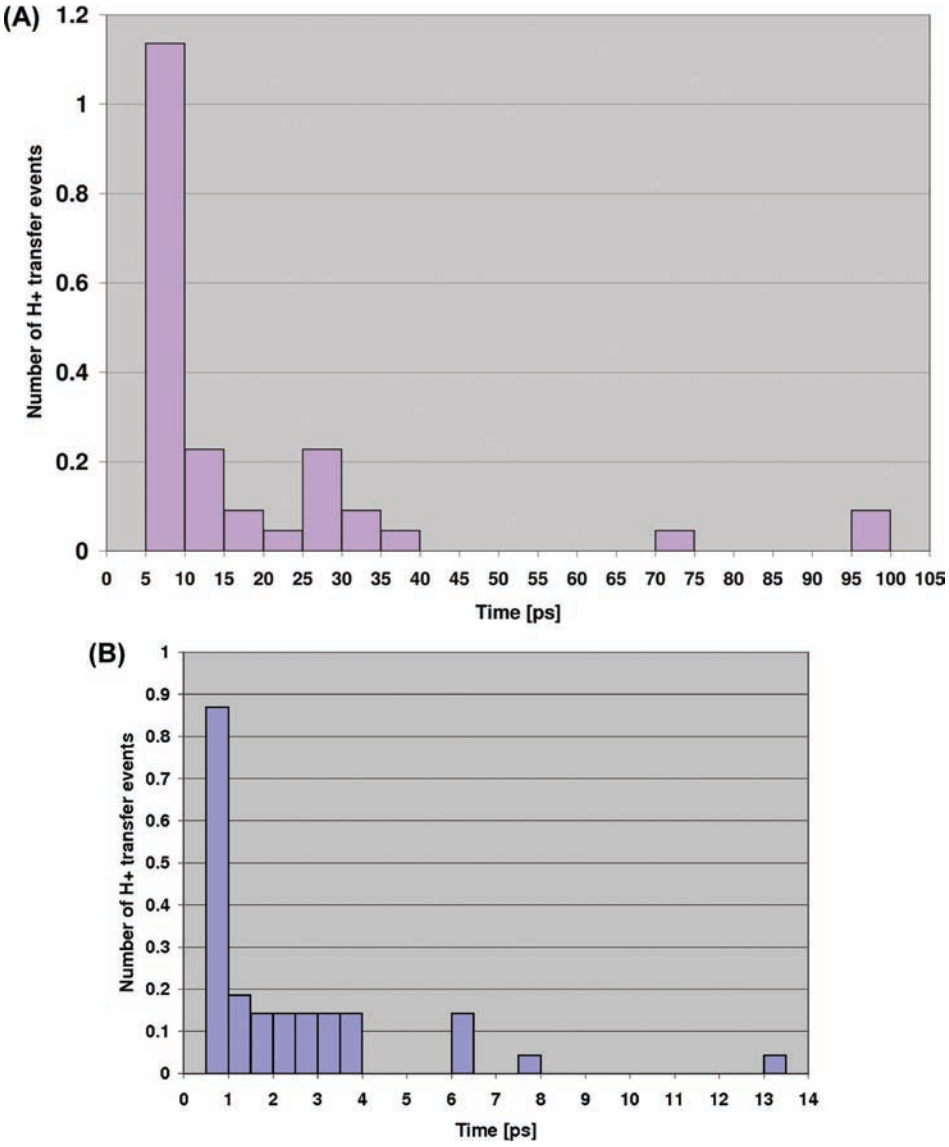

Figure 3. Number of H^+ transfer in conformer 1. (A) Conformer 1 OH stretch excitation. (B) Conformer 1 NH_3 (lysine) symmetrical stretch excitation. Each bar represents the averaged number of proton transfer seen during that time range (e.g., 0−5, 5−10, and 10−15 ps).

where P_j is the momentum value for mode j corresponding to the value Q_j of the coordinate. E_{jv} is the VSCF energy for level v of the mode j, while $\overline{V}_j(Q_j)$ is the VSCF effective potential for mode j.[60,61]

Our sampling of the initial conditions for trajectories for each conformer and type of excitation seems sufficient to reveal any major channel, though such sampling is not sufficient for finding minor products, which are statistically insignificant. All this, of course, is in the framework of the PM3 potential surfaces used. Finally, we note that the sampling used here assumes that the complex has no thermal energy prior to the excitation. The treatment can be extended to include thermal initial energy in a classical framework.

3. RESULTS AND DISCUSSION

3.1. Initial States—GlyLysH$^+$ Conformers. Five conformers of GlyLysH$^+$ were optimized by using the PM3 semiempirical electronic structure method. Figure 1 shows the minimized structures of these five conformers. Conformer 5, where the terminal NH_2 group of lysine is protonated, is the lowest minimum energy structure, and it is more stable than conformer 1, 2, 3, and 4 by 52.51, 5.25, 123.39, and 13.13 kJ/mol, respectively. Optimized structures of the five conformers calculated by the PM3 method were compared to these complexes obtained by MP2/DZV level of theory. Using MP2/DZV level of theory shows that conformer 5 is the lowest energy structure too and is more stable than conformer 1, 2, 3, and 4 by 15.75, 5.25, 149.65, and 7.88 kJ/mol, respectively.

Comparison of the optimized structures of the five conformers obtained by these two methods exhibits similar structural parameters. As seen from Table S1 (Supporting Information), the differences of bonds distance value and the angles values are fairly small. As noted previously, this supports the validity of PM3, at least for the present system.

3.2. The Dynamics of Proton Transfer. Following a selective excitation (of OH or of NH stretch) as done in previous experimental[62−64]and theoretical works,[61] a total number of

Table 1. Proton Transfer Pathways after Performing Vibrational Excitations[a]

pathway number	description of proton transfer pathway	C1 OH	C1 NH	C2 OH	C3 OH	C4 NH	C5 OH	C5 NH
1	lysine (NH_3) to glycine (OH)	7	16	11	7	8	11	17
2	internal (glycine)	4	_	6	13	10	6	4
3	(1) lysine (NH_3) to glycine (OH) (2) glycine to lysine (N to N terminal)	6	4	4	_	_	5	2
4	(1) glycine to lysine (N to N terminal) (2) lysine (the other NH_3^+) to glycine	2	1	_	_	_	_	_
5	(1) internal (glycine) (2) internal (lysine N to N)	3	_	1	_	_	_	_
6	(1) internal (lysine-N to N) (2) lysine to glycine	_	_	_	1	_	_	_
7	(1) internal (lysine-N to N) (2) internal (glycine)	_	_	_	1	_	_	_
8	(1) lysine to glycine (2) glycine to lysine (N to N not terminal)	_	2	_	_	3	1	_

[a] C1 is conformer 1, C2 is conformer 2, etc.

Table 2. Averaged First Proton Transfer and the Averaged Dissociation Times

conformer	average first proton transfer (ps)	average dissociation time (ps)
1 (OH)	9.73	22.55
1 (NH)	1.14	39.09
2 (OH)	15.00	42.42
3 (OH)	7.47	29.11
4 (NH)	19.98	44.09
5 (OH)	28.29	52.11
5 (NH)	13.13	53.33

eight different pathways of proton transfer were seen in the trajectories. In some trajectories, not a single proton transfer took place but a sequence of two proton transfers after which the species dissociated (a detailed discussion of the decomposition is given in the next subsection). Figure 2 illustrates some of the different pathways of proton transfers that were found during the dynamics in the different conformers. The proton transfer rate for conformer 1 can be seen in Figure 3. From this figure it is clear that there is selectivity in the proton transfer rate according to the type of excitation: In the OH stretch excitation, the highest rate of proton transfer was during the first 5 ps, while in the NH stretch excitation the highest rate was in the first 0.5 ps; therefore, it seems that proton transfer following NH excitation is much faster than that following OH excitation. The last proton transfers for the OH stretch excitation of conformer 1 took place more than 90 ps after excitation. On the other hand, for the NH stretch excitation of conformer 1, the last proton transfers were seen about 12.5−13 ps after excitation. Inspection of Figure 3 and Table 1 can shed some light on the appearance of the different proton transfer pathways according to the type of excitation performed: pathway 1 (lysine to glycine) was seen in all of the excitations, and in conformers 1, 2, and 5 this pathway was very dominant. One should also notice that in pathways 1 and 6, the excess proton is on glycine after the proton transfer, despite the low affinity of glycine for protons. Pathway 2 was witnessed in all of the excitations, except in the excitation of the NH stretch in conformer 1. Pathways 4−8 were much rarer, where pathways 4−7 were witnessed only in OH stretch excitations. Pathway 8 was witnessed both in OH and NH stretch excitations. In pathways 2−5, 7, and 8, glycine was in its neutral form after the proton transfer/s happened.

The time scales for the appearance of each proton transfer pathways are diverse, from less than 0.5 ps to over 100 ps; thus, the distribution of the time scales is very wide; e.g, pathway 1 was found in short times ($t \ll 1$ ps) and also in long times ($t > 50$ ps). Table 2 summarizes the averaged first proton transfer and the averaged dissociation times. The first proton transfer averaged time for each complex is in the range of a few picoseconds to 29 ps. This diverse range shows the sensitivity of the proton transfer to the initial conditions, since those proton transfer processes take place under conditions that lack statistical distribution.

In the OH stretch excitations (conformers 1−3 and 5) the first proton transfer occurred in a varied time table of a few picoseconds but not more than 100 ps. For the NH stretch excitations, the time scale for the first proton transfer is of tenths of picoseconds. The difference between the NH excitation and the OH excitation is thus large and systematic. The probable reason is just the role of geometry: for NH excitation, the proton is very near to the site of excitation. The proton transfer is then promoted directly by the supply of energy, well before vibrational energy redistribution.

3.3. Dynamics of Complex Dissociation. In all of the conformers and for each kind of vibrational excitation performed, the glycine and the lysine molecules moved away from one another, within a time of less than 160 ps, indicating the system was dissociating. Figure 4 shows the number of dissociation events versus time for excitations of the OH and the NH stretches in conformer 1. Dissociation of the system was defined by measuring the distance between selected atoms of glycine and selected atoms of lysine during the dynamics. When the distances between the selected atoms of glycine and lysine were above 125% of the initial distances, we considered it as a dissociation event (experience has shown that for such increased separation the process is irreversible). For the PM3 potential used, dissociation occurs also when the complex is at zero temperature prior to excitation, as assumed here. Addition of initial thermal energy may affect the dissociation times. While very accurate calculations of the energy difference between the complex and the

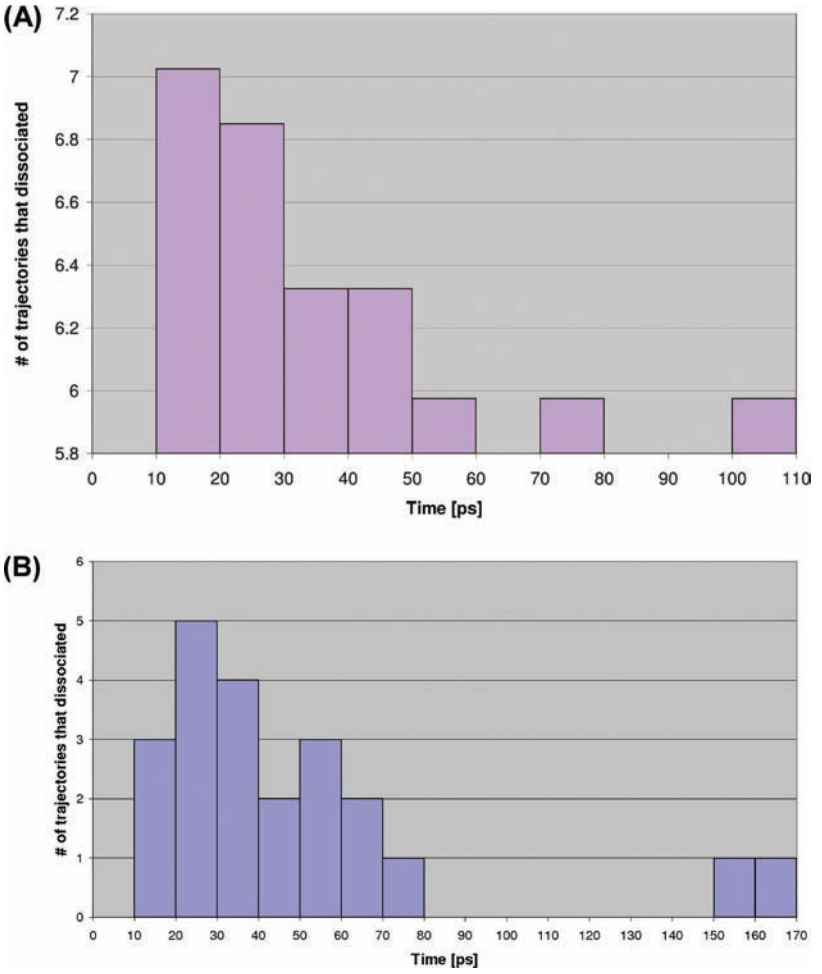

Figure 4. Dissociation time: (A) Conformer 1 OH stretch excitation. (B) Conformer 1 NH_3 asymmetrical stretch excitation. Each bar represents the number of trajectories for which dissociation of the system was seen during that time range (e.g., 0−10, 10−20, and 20−30 ps).

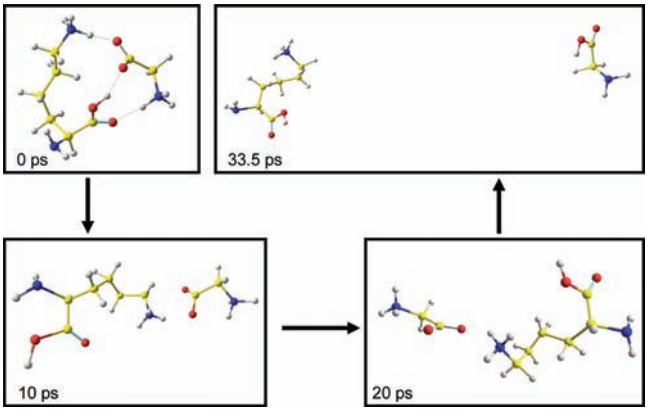

Figure 5. Four snapshots during dissociation of one of the trajectories of conformer 2.

dissociation fragments are very challenging [in view of the need of treating BSSE (basis set superposition error)] the energy for the v=1 OH excitation, combined with the thermal energy of the cluster, suffices for dissociation both at the MP2/DZV and B3LYP/CC-PVDZ levels.

Figure 5 illustrates four snapshots during dissociation of one of the trajectories of conformer 2.

In the OH stretch excitation (conformers 1−3 and 5) the decomposition occurred in most of the trajectories on the time scale of 10−140 ps. In the NH stretch excitation (conformers 1, 4, 5), decomposition was seen in most of the trajectories on the time scale of 10−160 ps and in one trajectory even after 340 ps. In both excitations (OH and NH stretch) for a few trajectories no decomposition was seen, and we assume that decomposition would have been reached eventually had we continued the dynamics for more time.

Excitations of both OH and NH stretches were studied for conformers 1 and 5. For conformer 1, the average dissociation time for OH excitation is about half than for the NH stretch excitation. For conformer 5, the mean dissociation time for OH excitation is also shorter than for the NH excitation, though in this case only moderately so. As seen in Figure 4 for conformer 1, the OH excitation leads to dissociation in 14 trajectories out of 30 in the first 30 ps. For the NH excitation in this case, only eight trajectories show dissociation in the first 30 ps. The excitation of the OH mode thus leads to faster dissociation than excitation of the NH mode. This is in accord with the experimental results of Oh et al.[30]

We fitted the results to exponential trend and the findings are as follows: The dissociation rates of the OH stretch excitation for conformers 1, 2, 3, and 5 are 0.039, 0.02, 0.041, and 0.025 ps^{-1},

correspondingly. The dissociation rates of the NH stretch excitation for conformers 1, 4, and 5 are 0.029, 0.024, and 0.009 ps^{-1}, correspondingly.

In Table 2, the averaged times of dissociation for the conformers are presented. The averaged dissociation time range is between ~22 and 53 ps. These large differences for the averaged dissociation time from different conformers strengthens the assumption of selectivity by the dissociation process. The dissociation occurred in all of the conformers 12−40 ps after the first proton transfer. We can attribute the upper range (after 40 ps dissociation) to the dissociation events that take place after a second proton transfer event. The selective behavior of the dissociation is compatible with the assumption that energy redistribution in the system is very incomplete at the time of dissociation. This should be due to the low threshold energy for dissociation in this system.

3.4. Conformational Changes. Conformational changes during dynamics were seen in all of the trajectories and for all the initial structures studied. On the other hand, in all trajectories, there was no event of transition between the initial minimum conformers to the other four minimum conformers found in this study. This fact can be explained by the relatively high energy of excitation, which enables the population of high energy structures. The dynamics is clearly not governed by the relative stability of the conformers, since much kinetic energy is available. In a previous study by Shmilovits-Ofir et al.[61] on the fundamental excitation of the OH stretch of the global minimum structure of glycine, it was found that an equilibrium-like ratio is established between the populations of the three lowest-lying conformers after about 10 ps. It seems that for the vibrationally excited proton-bound dimer, higher energy conformer structures are preferred in the course of the dynamics, possibly due to geometric factors (proximity to the excited structure).

4. CONCLUDING REMARKS

In this study, we explored the decomposition of $GlyLysH^+$ conformers and proton transfer induced by vibrational excitation of OH and NH stretching modes to the v=1 state. A realistic, though not accurate, potential surface was used, in the hope that the results may be typical of systems such as amino acids and peptides, which depend in particular on reasonable magnitudes for the barrier heights and couplings between the different modes.

The main findings of the simulations are as follows: First, proton transfer processes were found to be fast, on the picosecond time scale. The processes for the initial conditions needed are highly selective and nonstatistical. Indeed, mean proton transfer rates for different conformers differ considerably. Furthermore, there is a large difference between cases in which the N−H stretch is initially excited and those where the O−H stretch is promoted. Initial proton transfer rates for excited N−H stretch are about an order of magnitude faster than the corresponding rates for excited OH. This is likely to be due to the geometric proximity of the N−H local excitation to the proton site. Vibrationally induced proton transfer is so fast that energy redistribution cannot take place to a significant extent. The situation is very fast, for individual H^+ transfer events, for Rice−Ramsperger−Kassel−Marcus (RRKM) types of mechanisms to set in. This is also in line with the fact that the barriers for H^+ transfer in their system are low, certainly much lower than the hydrogenic stretch excitation energy. Dissociation following the vibrational stretch excitation is much slower than proton transfer. Mean dissociation times, in the range of 22−50 ps, are about an order of magnitude slower than mean H^+ transfer rates induced by OH excitation and nearly 2 orders of magnitude slower than initial H^+ transfer upon N−H stretch excitation also.

For dissociation our results show a substantial measure of selectivity and nonstatistical behavior. Only for the largest dissociation time scales seen in our simulations does it seem that RRKM types of treatment may apply. Vibrational stretch excitation is found to stimulate structural transitions. However, these do not seem to be limited to low-energy conformers or to be governed by preference for low-energy structures. The low energy barriers and the large excitation energy available are probably the key reasons. Finally, going back to the issue of proton transfer, the H^+ transfer in the small complex was found to follow about eight different pathways. The number of H^+ transfer pathways is thus appreciable but clearly much smaller than might be expected statistically. The processes are selective, but in a limited way. These considerations may apply at least in part to proton transfer in peptides and in proteins, and explorations of this should be of major interest. Further, it would be highly desirable to have real-time ultrafast experiments of the processes and mechanisms found, also for small complexes as studied here.

The results of the present study provide information on relevant rates of proton transfer, structural transitions, and dissociation that may be relevant also for charged peptides, at least semiquantitatively. The mechanisms and possibly the time scale of vibrational energy flow following excitation of OH stretches are potentially relevant for the very active experimental field of vibrational spectroscopy of biological molecules in the gas phase. The time scales and pathways of protein transfer and dissociation induced by vibrational excitation may also stimulate interest in differences or similarities with corresponding thermally induced processes in biological molecules in mass spectrometry.

■ ASSOCIATED CONTENT

Supporting Information. Table S1. This material is available free of charge via the Internet at http://pubs.acs.org.

■ AUTHOR INFORMATION

Corresponding Author
benny@fh.huji.ac.il

■ ACKNOWLEDGMENT

We thank Dr. Dorit Shemesh for helpful discussions during the writing of this paper. Advice from Dr. Brina Brauer on computational aspects is gratefully acknowledged. This research was supported in the framework of the Saeree K. and Louis P. Fiedler Chair in Chemistry at the Hebrew University.

■ REFERENCES

(1) Tunon, I.; Ruiz-Pernia, J. J.; Garcia-Viloca, M.; Bhattacharyya, S.; Gao, J. L.; Truhlar, D. G. *J. Am. Chem. Soc.* **2009**, *131*, 2687.
(2) Krimm, S.; Bandekar, J. *Adv. Protein Chem.* **1986**, *38*, 181.
(3) Torii, H.; Tasumi, M. *J. Chem. Phys.* **1992**, *96*, 3379.
(4) Herrmann, C.; Neugebauer, J.; Reiher, M. *New J. Chem.* **2007**, *31*, 818.

(5) Taillandier, E.; Peticolas, W. L.; Adam, S.; Huynhdinh, T.; Igolen, J. *Spectrochim. Acta Part A* **1990**, *46*, 107.
(6) Powell, J. W.; Peticolas, W. L.; Genzel, L. *J. Mol. Struct.* **1991**, *247*, 107.
(7) Fritzsche, H. *J. Mol. Struct.* **1991**, *242*, 245.
(8) Semenov, M.; Bolbukh, T.; Maleev, V. *J. Mol. Struct.* **1997**, *408*, 213.
(9) Bour, P.; Kubelka, J.; Keiderling, T. A. *Biopolymers* **2002**, *65*, 45.
(10) Stearns, J. A.; Seaiby, C.; Boyarkin, O. V.; Rizzo, T. R. *Phys. Chem. Chem. Phys.* **2009**, *11*, 125.
(11) Kamariotis, A.; Boyarkin, O. V.; Mercier, S. R.; Beck, R. D.; Bush, M. F.; Williams, E. R.; Rizzo, T. R. *J. Am. Chem. Soc.* **2006**, *128*, 905.
(12) Atkins, C. G.; Rajabi, K.; Gillis, E. A. L.; Fridgen, T. D. *J. Phys. Chem. A* **2008**, *112*, 10220.
(13) Adesokan, A. A.; Gerber, R. B. *J. Phys. Chem. A* **2009**, *113*, 1905.
(14) Graham, R. J.; Kroemer, R. T.; Mons, M.; Robertson, E. G.; Snoek, L. C.; Simons, J. P. *J. Phys. Chem. A* **1999**, *103*, 9706.
(15) Price, W. D.; Schnier, P. D.; Williams, E. R. *J. Phys. Chem. B* **1997**, *101*, 664.
(16) Julian, R. R.; Hodyss, R.; Beauchamp, J. L. *J. Am. Chem. Soc.* **2001**, *123*, 3577.
(17) Ko, C.; Levine, B.; Toniolo, A.; Manohar, L.; Olsen, S.; Werner, H. J.; Martinez, T. J. *J. Am. Chem. Soc.* **2003**, *125*, 12710.
(18) Price, W. D.; Jockusch, R. A.; Williams, E. R. *J. Am. Chem. Soc.* **1997**, *119*, 11988.
(19) Vendrell, O.; Gelabert, R.; Moreno, M.; Lluch, J. M. *J. Phys. Chem. B* **2008**, *112*, 5500.
(20) Pomes, R.; Roux, B. *Biophys. J.* **2002**, *82*, 2304.
(21) Pomes, R.; Roux, B. *Biophys. J.* **1996**, *71*, 19.
(22) Roux, B.; Nina, M.; Pomes, R.; Smith, J. C. *Biophys. J.* **1996**, *71*, 670.
(23) Pomes, R.; Roux, B. *J. Phys. Chem.* **1996**, *100*, 2519.
(24) Gaigeot, M. P. *Phys. Chem. Chem. Phys.* **2010**, *12*, 3336.
(25) Vaden, T. D.; de Boer, T. S. J. A.; Simons, J. P.; Snoek, L. C.; Suhai, S.; Paizs, B. *J. Phys. Chem. A* **2008**, *112*, 4608.
(26) Lucas, B.; Gregoire, G.; Lemaire, J.; Maitre, P.; Ortega, J. M.; Rupenyan, A.; Reimann, B.; Schermann, J. P.; Desfrancois, C. *Phys. Chem. Chem. Phys.* **2004**, *6*, 2659.
(27) Gregoire, G.; Gaigeot, M. P.; Marinica, D. C.; Lemaire, J.; Schermann, J. P.; Desfrancois, C. *Phys. Chem. Chem. Phys.* **2007**, *9*, 3082.
(28) Marinica, D. C.; Gregoire, G.; Desfrancois, C.; Schermann, J. P.; Borgis, D.; Gaigeot, M. P. *J. Phys. Chem. A* **2006**, *110*, 8802.
(29) Cimas, A.; Vaden, T. D.; de Boer, T. S. J. A.; Snoek, L. C.; Gaigeot, M. P. *J. Chem. Theory Comput.* **2009**, *5*, 1068.
(30) Oh, H. B.; Lin, C.; Hwang, H. Y.; Zhai, H. L.; Breuker, K.; Zabrouskov, V.; Carpenter, B. K.; McLafferty, F. W. *J. Am. Chem. Soc.* **2005**, *127*, 4076.
(31) Rajabi, K.; Fridgen, T. D. *J. Phys. Chem. A* **2008**, *112*, 23.
(32) Wyttenbach, T.; Witt, M.; Bowers, M. T. *Int. J. Mass Spectrom.* **1999**, *183*, 243.
(33) Jorgensen, W. L.; Tirado-Rives, J. *J. Am. Chem. Soc.* **1988**, *110*, 1657.
(34) Jorgensen, W. L.; Maxwell, D. S.; Tirado-Rives, J. *J. Am. Chem. Soc.* **1996**, *118*, 11225.
(35) Halgren, T. A. *J. Comput. Chem.* **1996**, *17*, 553.
(36) Halgren, T. A. *J. Comput. Chem.* **1996**, *17*, 490.
(37) Gerber, R. B.; Chaban, G. M.; Gregurick, S. K.; Brauer, B. *Biopolymers* **2003**, *68*, 370.
(38) Chaban, G. M.; Gerber, R. B. *J. Chem. Phys.* **2001**, *115*, 1340.
(39) Chaban, G. M.; Gerber, R. B.; Jung, J. O.; Gregurick, S. K. *Abstr. Pap. Am. Chem. Soc.* **2001**, *221*, U284.
(40) Brauer, B.; Chaban, G. M.; Gerber, R. B. *Phys. Chem. Chem. Phys.* **2004**, *6*, 2543.
(41) Shemesh, D.; Baer, R.; Seideman, T.; Gerber, R. B. *J. Chem. Phys.* **2005**, 122.
(42) Shemesh, D.; Chaban, G. M.; Gerber, R. B. *J. Phys. Chem. A* **2004**, *108*, 11477.
(43) Miller, Y.; Gerber, R. B. *J. Am. Chem. Soc.* **2006**, *128*, 9594.
(44) Shemesh, D.; Gerber, R. B. *J. Phys. Chem. A* **2006**, *110*, 8401.
(45) http://msg.chem.iastate.edu/gamess/
(46) Taketsugu, T.; Gordon, M. S. *J. Phys. Chem.* **1995**, *99*, 8462.
(47) Taketsugu, T.; Gordon, M. S. *J. Phys. Chem.* **1995**, *99*, 14597.
(48) Taketsugu, T.; Gordon, M. S. *J. Chem. Phys.* **1995**, *103*, 10042.
(49) Takata, I.; Taketsugu, T.; Hirao, K.; Gordon, M. S. *J. Chem. Phys.* **1998**, *109*, 4281.
(50) Gordon, M. S.; Chaban, G. M.; Taketsugu, T. *J. Phys. Chem.* **1996**, *100*, 11512.
(51) Maluendes, S. A.; Dupuis, M. *J. Chem. Phys.* **1990**, *93*, 5902.
(52) Stewart, J. J. P.; Davis, L. P.; Burggraf, L. W. *J. Comput. Chem.* **1987**, *8*, 1117.
(53) Chaban, G. M.; Jung, J. O.; Gerber, R. B. *J. Phys. Chem. A* **2000**, *104*, 2772.
(54) Chaban, G. M.; Jung, J. O.; Gerber, R. B. *J. Chem. Phys.* **1999**, *111*, 1823.
(55) Segev, B., *Phys. Rev. A* **2001**, *63*, 052114.
(56) Garcia-Vela, A. *Chem. Phys.* **2002**, *285*, 245.
(57) Wigner, E. *Phys. Rev.* **1932**, *40*, 749.
(58) Mccoy, A. B.; Hurwitz, Y.; Gerber, R. B. *J. Phys. Chem.* **1993**, *97*, 12516.
(59) Sun, L. P.; Hase, W. L. *J. Chem. Phys.* **2010**, 133.
(60) Miller, Y.; Chaban, G. M.; Finlayson-Pitts, B. J.; Gerber, R. B. *J. Phys. Chem. A* **2006**, *110*, 5342.
(61) Shmilovits-Ofir, M.; Miller, Y.; Gerber, R. B. *Phys. Chem. Chem. Phys.* **2011**, *13*, 8715.
(62) Dian, B. C.; Longarte, A.; Mercier, S.; Evans, D. A.; Wales, D. J.; Zwier, T. S. *J. Chem. Phys.* **2002**, *117*, 10688.
(63) Dian, B. C.; Longarte, A.; Winter, P. R.; Zwier, T. S. *J. Chem. Phys.* **2004**, *120*, 133.
(64) Dian, B. C.; Longarte, A.; Zwier, T. S. *Science* **2002**, *296*, 2369.